2009

The small heat-shock proteins HSPB2 and HSPB3 form well-defined heterooligomers in a unique 3 to 1 subunit ratio

J. den Engelsman
Radboud University, The Netherlands

S. Baros
Radboud University, The Netherlands

P. Y. W. Dankers
Radboud University, The Netherlands

B. Kamps
Radboud University, The Netherlands

W. T. Vree Egberts
Radboud University, The Netherlands

See next page for additional authors

The small heat-shock proteins HSPB2 and HSPB3 form well-defined heterooligomers in a unique 3 to 1 subunit ratio

Abstract

Various mammalian small heat-shock proteins (sHSPs) can interact with one another to form large polydisperse assemblies. In muscle cells, HSPB2/MKBP (myotonic dystrophy protein kinase-binding protein) and HSPB3 have been shown to form an independent complex. To date, the biochemical properties of this complex have not been thoroughly characterized. In this study, we show that recombinant HSPB2 and HSPB3 can be successfully purified from E.coli cells co-expressing both proteins. Nanoelectrospray ionization mass spectrometry and sedimentation velocity analytical ultracentrifugation analysis showed that HSPB2/B3 forms a series of well defined hetero-oligomers, consisting of 4, 8, 12, 16, 20 and 24 subunits, each maintaining a strict 3:1 HSPB2:HSPB3 subunit ratio. These complexes are thermally stable up to 40 °C, as determined by far-UV circular dichroism spectroscopy. Surprisingly, HSPB2/B3 exerted a poor chaperone-like and thermoprotective activity, which is likely related to the low surface hydrophobicity, as revealed by its interaction with the hydrophobic probe 1-anilino-8-naphthalenesulfonic acid. Co-immunoprecipitation experiments demonstrated that the HSPB2/B3 oligomer cannot interact with HSP20, HSP27 or αB-crystallin, whereas the homomeric form of HSPB2, thus not in complex with HSPB3, could efficiently associate with HSP20. Taken altogether, this study brings evidence that despite the high sequence homology within the sHSP family, the biochemical properties of the HSPB2/B3 complex are distinctly different from other sHSPs, indicating that the HSPB2/B3 assembly likely possesses other cellular functions than its family members.

Keywords

molecular chaperones, crystallin, small heat-shock protein, heterooligomers, MKBP

Disciplines

Biochemistry, Biophysics, and Structural Biology | Life Sciences | Physical Sciences and Mathematics | Social and Behavioral Sciences

Publication Details

This article was originally published as den Engelsman, J, Baros, S, Dankers, PYW, Kamps, B, Vree Egberts, WT, Bode, CS, Lane, LA, Aquilina, JA, Benesch, JLP, Robinson, CV, de Jong, WW, Boelens, WC, Journal of Molecular Biology, 393 (5), 1022-1032, 2009. Copyright Elsevier 2009. Original item available here

Authors

J. den Engelsman, S. Baros, P. Y. W. Dankers, B. Kamps, W. T. Vree Egberts, C. S. Bode, L. A. Lane, J. A. Aquilina, J. L. P. Benesch, C. V. Robinson, W. W. de Jong, and W. C. Boelens

THE SMALL HEAT SHOCK PROTEINS HSPB2 AND HSPB3 FORM WELL-DEFINED HETEROOLIGOMERS IN A UNIQUE 3 TO 1 SUBUNIT RATIO AND EXHIBIT A POOR CHAPERONE-LIKE ACTIVITY*

John den Engelsman[1], Sandor Boros[1], Patricia Y.W. Dankers[1], Bram Kamps[1], Wilma T. Vree Egberts[1], Csaba S. Böde[2], J. Andrew Aquilina[3], Justin Benesch [4], Carol V. Robinson[4], Wilfried W. de Jong[1] and Wilbert C. Boelens[1]

[1] Department of Biomolecular Chemistry 271, Nijmegen Center for Molecular Life Sciences, Radboud University, P.O. Box 9101, 6500 HB Nijmegen, The Netherlands. [2] Department of Biophysics and Radiation Biology, Semmelweis University, Budapest, Hungary. [3] School of Biological Sciences, University of Wollongong, Northfields Avenue, Wollongong, Australia. [4]Department of Chemistry, University of Cambridge, Lensfield Road, Cambridge, United Kingdom

Running Title: HSPB2 and HSPB3 form well-defined heterooligomers

Address correspondence to: Wilbert C. Boelens Ph.D. Department of Biomolecular Chemistry 271, Nijmegen Center for Molecular Life Sciences, Radboud University, P.O. Box 9101, 6500 HB Nijmegen, The Netherlands; Tel: +(31) 243616753, Fax: +(31) 243540525, E-mail: w.boelens@ncmls.ru.nl

Various mammalian small heat shock proteins (sHSPs) can interact with one another to form large polydisperse assemblies. In muscle cells, HSPB2/MKBP (myotonic dystrophy protein kinase-binding protein) and HSPB3 have been shown to form an independent complex. To date, the biochemical properties of this complex have not been thoroughly characterized. In this study, we show that recombinant HSPB2 and HSPB3 can be successfully purified from E.coli cells co-expressing both proteins. Nanoelectrospray ionization mass spectrometry and sedimentation velocity analytical ultracentrifugation analysis showed that HSPB2/B3 forms a series of well defined hetero-oligomers, consisting of 4, 8, 12, 16, 20 and 24 subunits, each maintains a strict 3:1 HSPB2:HSPB3 subunit ratio. Analyzing the thermal stability of the HSPB2/B3 assembly by far-UV circular dichroism spectroscopy revealed subtle structural changes, occurring slightly above 40 °C, and an unfolding curve with an inflection point at approximately 56 °C. Furthermore, HSPB2/B3 exerted poor chaperone-like and thermoprotective activity, which is likely related to the low surface hydrophobicity, as revealed by its interaction with the hydrophobic probe 1-anilino-8-naphthalenesulfonic acid. Finally, co-immunoprecipitation experiments demonstrated that the HSPB2/B3 oligomer does not interact with HSP20, HSP27 or αB-crystallin. However, HSPB2 that is not in complex with HSPB3 was found to efficiently associate with HSP20. Taken altogether, this study brings evidence that despite the high sequence homology of the subunits to other sHSPs, biochemical properties of the HSPB2/B3 complex are distinct different from other sHSP assemblies. Our results clearly demonstrate that HSPB2/B3 forms well-defined oligomeric complexes with poor chaperone-like activity.

INTRODUCTION

Small heat shock proteins (sHSPs) are molecular chaperones characterized by the presence of a conserved sequence of about 80-100 residues, referred to as the α-crystallin domain (for recent reviews see (1-3). This domain forms the C-terminal part of the protein, and is folded into a β-sandwich structure (4-6). The N-terminal part is more variable in both length and sequence, and largely determines the association properties of the homo- or heteromeric oligomers of sHSPs (7-9). The α-crystallin domain generally has a short and flexible C-terminal extension which modulates the chaperone-like activity, possessed by most sHSPs (10-12). sHSPs can form macromolecular associations up to 800 kDa, which readily dissociate and exchange subunits (13;14). *In vitro*, sHSPs typically display chaperone-like activities, measured by their ability to protect model substrates from thermally or chemically induced aggregation (15;16). *In vivo*, different sHSPs are implicated in an array of cellular processes, varying from muscle contraction, cell migration and cell survival to redox state and apoptosis (see reviews see (17-19)).

In human, ten members of the sHSP family have been recognized, formally designated as HSPB1-HSPB10 (20;21). While several sHSPs have extensively been studied, only limited information is available for HSPB2 (MKBP) and HSPB3 (22). HSPB2 and HSPB3 are mainly expressed in heart and skeletal muscle (23;24). In muscle extract HSPB2 and HSPB3 has been identified as a hetero-oligomer with an apparent molecular mass of 150 kDa. This sHSP complex has a more defined size than those formed by HSP27, αB-crystallin or HSP20, which can vary between 40 and 500 kDa (23). HSPB2 was initially discovered as a specific binding partner for myotonic dystrophy protein kinase (DMPK), hence its alternative name MKBP (DMPK-binding protein) (25). This interaction results in an enhanced kinase activity of DMPK and protects it from heat-induced inactivation (25). Association of HSPB2 with the outer membrane of mitochondria suggests a role in mitochondrial function (26;27). This might be related to the observed role of HSPB2 in the protection of the energy reserve; mice lacking HSPB2 have a higher rate of ATP loss during ischemic stress, and after ischemia the recovery of the energy level was slower (28). HSPB2 has been also implicated in the pathogenesis of diseases. In myotonic dystrophy diseased muscles, with reduced DMPK levels, an increased expression of HSPB2 is observed (25). Furthermore, HSPB2 can associate with the Aβ-containing plaques in Alzheimer's disease brains possibly preventing the pathogenic action of Aβ (29;30).

Less is known about HSPB3. Based on sequence prediction, HSPB3 was found to be the smallest member of the family with a 17 kDa monomeric size (31). A remarkable feature of HSPB3 is the lack of the C-terminal extension (31). In heart extracts, it exclusively interacts with HSPB2 (23), and upon proteasomal inhibition, ectopically overexpressed HSPB3 can translocate to the cytoskeleton in cultured rat cardiac H9C2 cells (32). Like HSPB2, the expression levels of HSPB3 are not upregulated upon heat shock (23).

Our goals in this study were two-fold: (1) to establish the stoichiometry of the oligomeric assembly of HSPB2/B3 and (2) to characterize the biochemical properties of the complex. We show that HSPB2 and HSPB3 form a series of complexes that are actually assemblies of tetrameric HSPB2/B3 complexes with a subunit ratio of 3:1. These oligomers were found to have poor chaperone and thermoprotective activity and are unable to interact with other sHSPs, such as HSP20, HSP27 and αB-crystallin.

EXPERIMENTAL PROCEDURES

Cloning, expression and purification

The cDNAs encoding for rat HSPB2 and rat HSPB3 were cloned into the pET3a expression vector by using the NdeI-BamHI sites and BglII-EcoRI sites, respectively. Protein expression was induced in the BL21 Rosetta strain, transformed with pET3a-HSPB2/B3, by addition of 350 μM isopropyl-β-D-thiogalactopyranoside and subsequent incubation for three hours at 37 °C. Cells were lysed by sonication in TEG buffer (25 mM Tris, pH 8.0, 2 mM ethylenediaminetetraacetic acid (EDTA), 50 mM glucose) and then centrifuged at 16,000 × g for 45 min at 4°C. The obtained supernatants were subjected to 0.12% polyethylene-imine precipitation. SHSPs were first fractionated on a DEAE–Sepharose column, using a gradient from 0 to 1 M NaCl in 25 mM bis-Tris pH 6.35, 2 mM EDTA, and after desalting further fractionated on a Source 15Q HR 16/10 column using the same salt gradient. This yielded fractions containing both HSPB2 and HSPB3, and HSPB2 alone. Recombinant HSP27, HSP20 and αB-crystallin were purified in a similar manner, using pET3a-human-HSP27, pET8c-rat-HSP20 and pET3b-human-αB-crystallin as described previously (33).

SEC-MALLS

SEC-MALLS analyses were performed by chromatographic separation of samples (100 μg), on an Agilent 1200 system, using a TSK-Gel3000SW column (TOSOH-BIOSEP) at a flow rate of 0.5 mL/min in 10 mM sodium citrate, pH 6.25, 100 mM NaCl. MALLS analysis of a sample was performed continuously on the column eluate, as it passed through a triple-angle miniDAWN™ TREOS light scattering detector in series with an Optilab rEX refractive index instrument (both from Wyatt Technologies, Inc). Data were analyzed using Astra v5.3.2, a dn/dc value of 0.185, an A_2 value of 0, and a 1st order Zimm fit.

Far-UV circular dichroism spectroscopy

CD-spectra were recorded on a J-810 spectropolarimeter (Jasco) in a 1 mm cuvette using 250 μg/mL of HSPB2/B3 dialyzed against 10 mM potassium phosphate buffer pH 7.8. Spectra of HSPB2/B3 and buffer alone were recorded between 195 and 250 nm with a scanning speed of 20 nm/min with a response time of 1 second and a bandwidth set to 1 nm. To determine the heat stability, the temperature of the cuvette was increased from 20 °C up to 80 °C with 1 °C /min. After each increment of 2 °C 15 spectra were recorded and averaged. The spectra of HSPB2/B3 were corrected for the spectra of the buffer at the corresponding temperatures.

Mass spectrometry

HSPB2/B3 was buffer exchanged from the initial buffer into200 mM ammonium acetate, pH 6.8, using a Superdex 200 column on an AKTA prime FPLC and subsequently separated into two fractions, A and B, on a Superose 6 column. From these fractions nanoelectrospray mass spectra were acquired using a Qstar XL mass spectrometer (MDS Sciex), under conditions optimized for the transmission of non-covalent protein complex interactions, using a previously described protocol (34). Typical instrument parameters in positive ion mode, were: ion spray voltage 1.2 kV, declustering potential 100 - 150 V, focusing potential 100 V, declustering potential 2 15V, quadrupole voltage (Q0) 50 V, collision gas (CAD) 6, ion release delay 6 and ion release width 5. Experiments were acquired at instrument base pressure of 6.5 mbar.

Analytical ultracentrifugation

Samples were placed in assembled cells with sapphire windows and 12-mm path length centerpieces, which were made of charcoal-filled epon, and were centrifuged at 42,000 rpm in an eight-holed An50-Ti rotor. The data were collected using the absorption detection system of the XL-I analytical ultracentrifuge (Beckman Coulter) at 276 nm. The cells were aligned

manually, the inner cell housing scribe line on the bottom of the cell was visually aligned with the inner rotor hole scribe lines. Once the vacuum was less than 5 μm, the rotor was allowed to reach the set temperature of 22 °C and then was equilibrated for 1 hour before accelerating the rotor to the maximum speed of 42,000 rpm. The cells were scanned at 276 nm as frequently as possible, using a radial increment of 0.003 cm. At the end of the experiment, the data were analyzed by Sedfit (35).

The $c(s)$ continuous distribution model was used with input parameters that include radial position for the cell bottom and initial position for the meniscus, an initial estimate of frictional coefficient ratio (f/f_0) of 1.2, the radial data range and sedimentation coefficient range (0.5-20 S, the resolution was set at 200) for fitting. The solvent density and viscosity as well as the partial specific volume were calculated using the public domain software program Sednterp (36). The calculated partial specific volume of the HSPB2/B3 oligomer was corrected for the subunit ratio of 3:1. An initial $c(s)$ distribution was generated using these parameters. Subsequently, it was optimized using the meniscus position and f/f_0 as floating parameters. Using the integration tool provided in Sedfit, the relative concentration and weight average sedimentation coefficients were determined for each species. In all cases regularization with Tikhonov-Phillips obtained the best results. The root mean square deviation (rmsd) for all analysis was < 0.004.

ANS binding

To study the binding of the hydrophobic probe 1-anilino-8-naphthalenesulfonic acid (ANS), 10 μM HSPB2/B3 in 10 mM sodium phosphate buffer (pH 7.4) containing 100 mM NaCl and 500 mM ANS in methanolic solution was used to make a series of mixtures with different molar ratio's. The mixtures were incubated for 10 min at 37 °C after which the fluorescence emission was measured at 490 nm using an excitation wavelength of 390 nm.

Chaperone assays

To measure the chaperone-like properties of sHSPs the insulin protection assay described by Farahbakhsh *et al.* (37) and the citrate synthase (CS) assay described by Kappé *et al.* (38) were used. Briefly, for the insulin protection assay the proteins were dialyzed overnight at 4 °C against buffer containing 20 mM sodium phosphate, pH 6.9, and 20 mM Na_2SO_4. In a final volume of 1 mL, 250 μg HSPB2/B3 or αB-crystallin was incubated with 250 μg bovine insulin (Sigma) at 40 °C for 5 minutes. The denaturation of insulin was initiated by adding 3 mg dithiothreitol (DTT), and absorbance was measured at 360 nm for 15 minutes at 40 °C in a Perkin Elmer Lambda 2 UV/VIS spectrophotometer. For the CS protection assay the proteins were dialyzed overnight at 4 °C against 40 mM Hepes-KOH, pH 7.5. 70 μg sHSP was incubated at 44 °C for 5 minutes. After adding 70 mg CS to a total volume of 1 mL the heat induced denaturation of the substrate was followed at 44 °C by measuring the turbidity at 360 nm for 45 minutes in a Perkin Elmer Lambda 2 UV/VIS spectrophotometer.

Colony Survival Assay

Cells transformed with the appropriate bacterial expression construct were first grown overnight. All cell suspensions were then diluted to OD_{580} = 0.6, and protein expression was induced for 1 hour by adding 350 μM isopropyl-β-D-thiogalactopyranoside. After induction cells were heat-shocked at 48 °C for 60 minutes, after which the cell cultures were diluted to OD_{580} = 0.06. The recovery was monitored during 4.5 hour at 37 °C by measuring the increase of OD_{580} at 30 minute time intervals.

Co-immunoprecipitation assay

Purified HSPB2/B3 (1 μg) and HSPB2 (0.5 μg) were incubated either alone (negative control) or together with HSP20, HSP27, αB-

crystallin (5 μg) or a mixture of the three proteins (each 5 μg) in TEN buffer (25 mM Tris pH 8.0, 100 mM NaCl, 2 mM EDTA and 0.05% NP40) for 60 minutes at room temperature. After the incubation, antibodies directed against HSPB2, HSP20, αB-crystallin (all three raised in rabbits) or HSP27 (Stressgen) coupled to protein A beads (Roche) were added to the indicated mixtures and rotated for 60 minutes. The beads were then pelleted and washed 3 times with 1 mL TEN buffer. The proteins bound to the beads were separated by SDS-PAGE and analyzed by Western blotting.

RESULTS

HSPB2 together with HSPB3 forms heterooligomeric complexes

Initially, it was attempted to express and purify HSPB2 and HSPB3 separately in order to study their properties and to characterize the HSPB2/B3 complex. Although separate expression of both proteins was adequate, purification and stability turned out to be unsatisfactory under a variety of conditions. Co-expression of HSPB2 with HSPB3 already allowed the formation of the complex in *E. coli*, and from the extract of those cells HSPB2/B3 could successfully be purified by ion exchange chromatography. In the initial DEAE step, HSPB2 eluted at low salt concentrations together with HSPB3 in a certain ratio. At higher salt concentrations, HSPB2 eluted mainly without HSPB3 (Fig. 1A), indicating that *E. coli* expressed an excess of HSPB2 compared to HSPB3. Unfortunately, HSPB2 was only stable in a diluted form and started to precipitate as soon as the concentration was increased. Due to this behavior the biochemical properties of HSPB2 on its own could not be analyzed. Fractions containing both HSPB2 and HSPB3 were pooled and further purified on a Source Q column. The obtained HSPB2 and HSPB3 were concentrated in 20 mM phosphate buffer pH 7.5 with 100 mM NaCl and 2 mM EDTA to a concentration of 15 mg/mL (0.77 mM). This solution was subsequently diluted into 1 mg/mL final concentration and analyzed by size exclusion chromatography coupled with multi-angle laser light scattering (SEC-MALLS). In the obtained chromatogram HSPB2/B3 appeared in three peaks; a major peak A and a smaller peak B, which is poorly separated from a third peak C (Fig. 1B). Based on the MALLS measurements, the molecular masses of the HSPB2/B3 complexes in peaks A and B are 78 and 166 kDa, respectively. Peak C contains several high molecular weight complexes with masses ranging from 250 to 300 kDa.

HSPB2/B3 forms hetero-oligomeric complexes with a fixed subunit ratio

To further characterize the HSPB2/B3 oligomers, the complexes were analyzed by nano-ESI-MS under conditions that preserve non-covalent interactions (39). The unprecedented accuracy of this technique can be used to calculate the exact subunit stoichiometry of the hetero-oligomers. Prior to mass spectrometry, the proteins were separated on a Superose 6 column, using a 200 mM ammonium acetate buffer at pH 6.8, which gave a similar elution pattern with two relatively sharp peaks A and B, and a broader peak C (Fig. 2A). This broadness is likely caused by the mass variations of the large complexes shown by the MALLS measurements (Fig. 1B). Mass spectra were collected for oligomeric HSPB2/B3 present in peak A and peak B containing a fraction of peak C. Analysis of peak A (Fig. 2B) revealed an intense series of peaks (T) between *m/z* 3,500-5,250, which were found to arise from an HSPB2/B3 complex with a mass of 77,887 ± 34 Da. According to the mass this is a tetrameric complex (T, 4-mer) composed of three HSPB2 subunits (calculated mass 20,235 Da) and one HSPB3 subunit (calculated mass 16,968 Da). A low intensity charge state series between *m/z* 1,500-3,200 could be observed (insert to panel

B), which arise from three different species: HSPB3 monomer with a mass of 17,024 ±1 Da, a heterodimer (heteroD) with a mass of 37,294 ± 9 Da (calculated mass 37,203 Da), and a HSPB2 homodimer (homoD) with a mass of 40,458 ±39 Da (calculated mass 40,470 Da). The predominant charge state series found in peak B (Fig. 2C) corresponds with the mass of an octamer (O, 8-mer) being 155,696 ±53 Da composed of six HSPB2 and two HSPB3 subunits. The next most intense peak series in this spectrum (mass 467,588 ±127 Da) corresponds to a 24-mer and has the same 3:1 subunit ratio observed in case of the tetra- and octa-meric complexes. A low intensity charge state series between *m/z* 5800-8000 (insert to panel C) was found to arise from a dodecamer oligomer (DoD, 12-mer) with a mass of 233,767 ± 94 and another low intensity series arises from a hexadecamer (hexD, 16 mer) with a mass of 311,853 ±19 Da. Both the dodecamer and hexadecamer conform to the same subunit ratio observed for the tetramer, octamer and 24-mer.

In order to determine the relative amount of each oligomeric complex, a sedimentation velocity centrifugation analysis, using an analytical ultracentrifuge (Experimental Procedures) was performed. By employing the *c(s)* continuous distribution model, 7 different complexes varying in sedimentation rate between 4.6 and 19.4 S were identified (Fig. 3). Based on the calculated molecular masses of these complexes (Table 1), 5 of these complexes have been identified by nano-ESI-MS as being 4-, 8-, 12-, 16- and 24-mer. Also a complex with the mass of a 20-mer could be detected, which was not observed by nano-ESI-MS, likely because of its low abundance. Beside these complexes, also a large complex with a mass of 638,000 Da was detected by analytical ultracentrifugation, but the accuracy of this mass was not sufficient to determine if this complex belongs to the series of well-defined oligomers. By analyzing the peak areas we determined the relative amount of each oligomer (Table 1). The heterotetramer (4-mer) forms more than 60% of the amount of all species, indicating that this oligomer is the predominant form.

Heat-induced structural changes of HSPB2/B3

The chaperone-like activity of sHSPs is likely modulated by structural changes in response to stress, such as elevated temperatures (40). To assess heat-induced structural changes of HSPB2/B3 a series of far-UV circular dichroism (CD) spectra were recorded at temperatures ranging from 20 till 80 degrees. The CD spectra for HSPB2/B3 recorded between 20 and 40 °C were quite similar and showed a relatively broad minimum around 215 nm (Fig. 4A). Above 40 °C, a change in the spectra was observed, and found to be most pronounced at 204 nm. At this wavelength the negative ellipticity is characteristic for random coil structures caused by the unfolding of the subunits (41). This negative ellipticity at 204 nm slightly increased at temperatures ranging from 40 to 50 °C and strongly increased between 50 and 64 degrees, with an inflection point of the unfolding curve at 56 degrees (Fig. 4B).

Surface hydrophobicity of HSPB2/B3

The surface hydrophobicity of HSPB2/B3 was compared with that of αB-crystallin. αB-crystallin has a strong affinity for unfolding proteins, which correlates well to the surface hydrophobicity of this sHSP (42). The surface hydrophobicity was measured with the hydrophobic probe ANS, a fluorescence dye with increasing fluorescence intensity upon binding to exposed hydrophobic surfaces. The fluorescence intensity was measured at different ANS to protein molar ratios (Fig. 5). Remarkably, for HSPB2/B3 very little fluorescent ANS signal was recorded, even at high molar ratios, showing that, compared to αB-crystallin, HSPB2/B3 exhibits very low ANS binding capacity. This indicates that the

surface of HSPB2/B3 is relatively non-hydrophobic.

HSPB2/B3 has poor chaperone-like and thermoprotective activity

A low surface hydrophobicity is an indication for a poor chaperone-like activity. To study the chaperone-like activity of HSPB2/B3 three different chaperone assays were used (Fig. 6). In the first assay the ability to prevent aggregation of dithiothreitol-denatured insulin was measured. In line with previous data (37), recombinant αB-crystallin fully inhibited the DTT-induced aggregation of insulin at a 1-to-1 mass ratio (Fig. 6A). Conversely, practically no prevention of insulin aggregation was observed in the presence of HSPB2/B3. In the second assay the ability to prevent the heat-induced aggregation of citrate synthase (CS) was assessed (38). At a 1-to-1 mass ratio both HSPB2/B3 and αB-crystallin were able to prevent CS aggregation, although HSPB2/B3 showed significantly less chaperone-like activity than αB-crystallin (Fig. 6B). In the third assay, the ability of HSPB2/B3 to confer thermotolerance to *E. coli* cells was established (Fig. 6C). *E. coli* cells expressing HSPB2/B3, αB-crystallin or the chaperone-like activity lacking negative control βB2-crystallin (43), were heat shocked for 60 minutes at 48 °C, a temperature at which marginal unfolding of HSPB2/B3 was detected (Fig. 4B). After heat shock, cells were diluted in fresh medium and cell recovery at 37 °C was monitored for 4.5 hours, by measuring the cell density (OD_{580}) at 30 minutes intervals. After 4.5 hours, a considerable growth recovery of αB-crystallin expressing cells was observed, while cells expressing HSPB2/B3 or the control protein were still not recovered. These results show that HSPB2/B3 has no (Figs 6A and C) or only little (Fig. 6B) chaperone-like and thermoprotective activity as compared to αB-crystallin.

Interaction of HSPB2/B3 with other sHSPs

Although the HSPB2/B3 association in muscle cell extracts has been suggested to act mainly as an independent sHSP complex since it does not associate with HSP27 and αB-crystallin, a weak interaction between HSP20 and HSPB2 has been detected (23). To analyze whether the recombinant HSPB2/B3 oligomeric complexes exhibit similar associating properties, a mixture containing equal amounts of purified HSP20, HSP27 and αB-crystallin was allowed to exchange subunits with HSPB2/B3. In this experiment purified HSPB2 was used, which in the diluted form remained soluble during co-immunoprecipitation. After 60 min of incubation at room temperature HSPB2 was immunoprecipitated with HSPB2 antiserum followed by Western blot analysis to detect the interacting proteins (Fig. 7A). As expected, HSPB3 was efficiently co-precipitated with HSPB2 (Fig. 7A lanes 4 and 6). Interestingly, HSP20 did not co-precipitate with HSPB2/B3, but was efficiently pulled down with HSPB2, while αB-crystallin and HSP27 co-precipitated neither with HSPB2/B3 nor HSPB2 (compare lanes 5 and 6).

In the reciprocal pull-down experiment specific antibodies directed to HSP20, HSP27 and αB-crystallin were used for the immoprecipitation and co-precipitated HSPB2 was detected by Western blot analysis (Fig. 7B). The three sHSPs were incubated with HSPB2/B3 or HSPB2 either individually (Fig. 7B lanes 3-4) or as a mixture (Fig. 7B lanes 5-6). Again, only HSP20 showed a clear interaction with HSPB2, but not with HSPB2/B3. No quantitative differences of co-precipitated HSPB2 were observed in the presence of HSP27 and αB-crystallin, indicating that the interaction between HSP20 and HSPB2 is not affected by these two sHSPs. These results show that the HSPB2/B3 complex does not interact with

HSP20, HSP27 or αB-crystallin, while HSPB2 can indeed form a complex with HSP20.

DISCUSSION

We succeeded to co-express HSPB2 and HSPB3 as reported in this study, and purified the oligomeric complex of HSPB2/B3. Interestingly, HSPB3 was only detected as a component of this complex, while HSPB2 could also be isolated as a separate homomeric assembly, albeit in a poorly soluble form. Analysis of the recombinant HSPB2/B3 complex by advanced methods such as SEC-MALLS, Nano-ESI-MS and sedimentation velocity centrifugation revealed the presence of a series of heteromeric oligomers. The masses of these oligomers varied from 77,897 up to 467,588 Da, corresponding to assemblies containing 1 to 6 tetramers, each comprising three HSPB2 and one HSPB3 subunits (Table 1). The tetramer is the most abundant oligomeric species that can be formed by HSPB2 and HSPB3. Based on the mass differences between the higher oligomers, this structure is the building block for the large HSPB2/B3 complexes. The 24-mer is likely a more stable structure compared to the other higher oligomers, since this complex is relatively more pronounced as determined by both nano-ESI-MS (Fig. 2C) and sedimentation analysis (compare ratio amount n+4- and n-mer in Table 1). The organization of HSPB2/B3 in distinct oligomeric structures is a very conspicuous feature, which to our knowledge, is a feature that has never been observed for other sHSPs.

By Nano-ESI-MS, small amounts of HSPB2 homodimers and HSPB2/B3 heterodimers have been detected (Fig. 2A). This observation allowed to draw the conclusion that the tetramer is composed of dimeric units. Such dimeric "building blocks" have been suggested as being a common feature of sHSPs (1;44). In this case, the tetramer is formed by the association of one homodimer and one heterodimer. This fits with the yeast two hybrid data showing that HSPB2 interacts with both itself and HSPB3, while HSPB3 can only interact with HSPB2 and not itself (23).

Based on the SEC analysis in this study, in agreement with earlier reports (23;25;45), the main HSPB2/B3 complex was estimated to be in the range of an octamer, 150 kDa (Fig. 2A, peak A). However, this is twice as large as found by mass spectrometry, MALLS and sedimentation velocity centrifugation analysis (Fig. 1 and 2B). This indicates that HSPB2/B3 elutes faster from a size exclusion column than expected. A possible explanation for this aberrant behavior could be the presence of extra space inside the complex, as has been observed for HSP26 (46).

By heat-induced denaturation we found that HSPB2/B3 forms a relatively stable structure, which only at temperature around 56 °C forms extensive random coil structures. However, the unfolding starts already at 40 °C, which suggests that at this temperature structural changes already occur. Such structural changes, close to physiological temperatures have been also described for other sHSPs, and thus might be an important mechanism to regulate the chaperone-like activity (40).

Previously, it was shown that the α-crystallin domain is needed to form the dimer structures, while the N-terminal and C-terminal tails are mainly involved in stabilizing the quaternary structure (44). The C-terminal extensions can form critical bridges between neighboring subunits via a conserved IXI/V sequence (12). The C-terminal extension of HSPB2 does not contain this conserved sequence but, based on its length, it could still be involved in stabilizing the quaternary structure. However, HSPB3 has an extension of about 5 residues long, which is likely too short to form a bridge between adjacent α-crystallin domain dimers. The absence of a long C-terminal extension in HSPB3 might be an important factor for the unique nature of the HSPB2/B3

complex to form tetramers that can subsequently assemble into multiple oligomers.

sHSPs expressed in the same cell often form heteromeric complexes consisting of several sHSPs, such as those described for αB-crystallin and HSP27 (47). There are also examples in which more than one type of sHSP oligomeric complexes can actually exist in the cytoplasm of a single cell. In higher plants, class I and II sHSPs are such proteins that can be found in separate oligomers (48). HSPB2 and HSPB3 also form separate oligomers, despite their co-expression with e.g. HSP27, HSP20 and αB-crystallin in muscle cells. Interestingly, HSP20 is able to interact with HSPB2 (23), which raised the question whether HSP20 can also interact with HSPB2 as part of the HSPB2/B3 complex. By co-immunoprecipitation experiments we have shown that the HSPB2/B3 complex does not interact with HSP20 (Fig. 7). Only HSPB2 alone, thus not in complex with HSPB3, binds relatively well to HSP20. These data show that HSPB2/B3 is indeed a separate complex not able to interact with other sHSPs. This is in good agreement with the yeast two-hybrid studies showing that only HSP20 and HSPB3 are able to interact with HSPB2 (23). Recently, HSPB2 has been found to also interact with HSPB8 (HSP22) (49). The concentration of HSPB2 and HSPB3 in rat skeletal muscle extract was found to be 0.30 and 0.09 μg/mg of total protein, respectively (23). Thus the ratio of expression between the two proteins is close to 3:1, which suggest that almost all HSPB2 will be present in the HSPB2/B3 complex. This may explain why in muscle tissue extract only a minor fraction of HSPB2 associates with HSP20 (23).

HSPB2/B3 hardly binds ANS (Fig. 5), indicating that the surface of the complex is not very hydrophobic. The low surface hydrophobicity is likely to affect the binding of unfolding proteins (50), and this way, it can contribute to the observed poor chaperone-like activity of the HSPB2/B3 complex. Interestingly, purified homomeric HSPB2 has been shown to have chaperone-like activity that protects the kinase DMPK from heat-induced inactivation (25). By using a diluted preparation of purified HSPB2, we could also detect a moderate chaperone-like activity of HSPB2 for insulin (data not shown). It is thus possible that HSPB3, at least in part, is responsible for the low chaperone-like activity of the HSPB2/B3 complex. Therefore, HSPB2/B3 may function as an inactive storage complex from which HSPB2 has to dissociate in order to become active. However, the relation between *in vitro* and *in vivo* chaperone-like activity does not always correlate (51) and thus care must be taken to extrapolate the *in vitro* data. It remains possible that HSPB2/B3 function as a chaperone complex *in vivo* only dedicated to specific substrates.

In summary, the results indicate that HSPB2/B3 forms a series of heterooligomers with a well-defined subunit ratio and differ in number of tetramers. They have poor chaperoning activity and do not interact with other sHSPs, which is atypical compared to other sHSPs. Further studies are needed to understand the structural and cellular functions of this complex.

Reference List

1. Haslbeck, M., Franzmann, T., Weinfurtner, D., and Buchner, J. (2005) *Nat.Struct.Mol.Biol.* **12,** 842-846

2. Sun, Y. and Macrae, T. H. (2005) *Cell Mol.Life Sci.* **62,** 2460-2476

3. Taylor, R. P. and Benjamin, I. J. (2005) *J Mol.Cell Cardiol.* **38,** 433-444

4. Kim, K. K., Kim, R., and Kim, S. H. (1998) *Nature* **394,** 595-599

5. Stamler, R., Kappe, G., Boelens, W., and Slingsby, C. (2005) *J Mol.Biol.* **353,** 68-79

6. Van Montfort, R. L., Basha, E., Friedrich, K. L., Slingsby, C., and Vierling, E. (2001) *Nat.Struct.Biol.* **8,** 1025-1030

7. Pasta, S. Y., Raman, B., Ramakrishna, T., and Rao, C. (2003) *J Biol.Chem.* **278,** 51159-51166

8. Stromer, T., Fischer, E., Richter, K., Haslbeck, M., and Buchner, J. (2004) *J Biol.Chem.* **279,** 11222-11228

9. Theriault, J. R., Lambert, H., Chavez-Zobel, A. T., Charest, G., Lavigne, P., and Landry, J. (2004) *J Biol.Chem.* **279,** 23463-23471

10. Carver, J. A. (1999) *Prog.Retin.Eye Res.* **18,** 431-462

11. Li, Y., Schmitz, K. R., Salerno, J. C., and Koretz, J. F. (2007) *Mol.Vis.* **13,** 1758-1768

12. Saji, H., Iizuka, R., Yoshida, T., Abe, T., Kidokoro, S., Ishii, N., and Yohda, M. (2008) *Proteins* **71,** 771-782

13. Aquilina, J. A., Benesch, J. L., Bateman, O. A., Slingsby, C., and Robinson, C. V. (2003) *Proc.Natl.Acad.Sci.U.S.A* **100,** 10611-10616

14. Bova, M. P., Mchaourab, H. S., Han, Y., and Fung, B. K. (2000) *J Biol.Chem.* **275,** 1035-1042

15. Horwitz, J. (1992) *Proc.Natl.Acad.Sci.U.S.A* **89,** 10449-10453

16. Jakob, U., Gaestel, M., Engel, K., and Buchner, J. (1993) *J Biol.Chem.* **268,** 1517-1520

17. Arrigo, A. P., Simon, S., Gibert, B., Kretz-Remy, C., Nivon, M., Czekalla, A., Guillet, D., Moulin, M., Diaz-Latoud, C., and Vicart, P. (2007) *FEBS Lett.* **581,** 3665-3674

18. Fan, G. C., Chu, G., and Kranias, E. G. (2005) *Trends Cardiovasc.Med.* **15,** 138-141

19. Shemetov, A. A., Seit-Nebi, A. S., and Gusev, N. B. (2008) *J Neurosci.Res.* **86,** 264-269

20. Fontaine, J. M., Rest, J. S., Welsh, M. J., and Benndorf, R. (2003) *Cell Stress.Chaperones.* **8,** 62-69

21. Kappe, G., Franck, E., Verschuure, P., Boelens, W. C., Leunissen, J. A., and de Jong, W. W. (2003) *Cell Stress.Chaperones.* **8,** 53-61

22. Hu, Z., Yang, B., Lu, W., Zhou, W., Zeng, L., Li, T., and Wang, X. (2008) *J Neurosci.Res.* **86,** 2125-2133

23. Sugiyama, Y., Suzuki, A., Kishikawa, M., Akutsu, R., Hirose, T., Waye, M. M., Tsui, S. K., Yoshida, S., and Ohno, S. (2000) *J Biol.Chem.* **275,** 1095-1104

24. Verschuure, P., Tatard, C., Boelens, W. C., Grongnet, J. F., and David, J. C. (2003) *Eur.J Cell Biol.* **82,** 523-530

25. Suzuki, A., Sugiyama, Y., Hayashi, Y., Nyu-i N, Yoshida, M., Nonaka, I., Ishiura, S., Arahata, K., and Ohno, S. (1998) *J Cell Biol.* **140,** 1113-1124

26. Kadono, T., Zhang, X. Q., Srinivasan, S., Ishida, H., Barry, W. H., and Benjamin, I. J. (2006) *J Mol.Cell Cardiol.* **40,** 783-789

27. Nakagawa, M., Tsujimoto, N., Nakagawa, H., Iwaki, T., Fukumaki, Y., and Iwaki, A. (2001) *Exp.Cell Res.* **271,** 161-168

28. Pinz, I., Robbins, J., Rajasekaran, N. S., Benjamin, I. J., and Ingwall, J. S. (2008) *FASEB J* **22,** 84-92

29. Wilhelmus, M. M., Otte-Holler, I., Wesseling, P., de Waal, R. M., Boelens, W. C., and Verbeek, M. M. (2006) *Neuropathol.Appl.Neurobiol.* **32,** 119-130

30. Wilhelmus, M. M., Boelens, W. C., Otte-Holler, I., Kamps, B., de Waal, R. M., and Verbeek, M. M. (2006) *Brain Res.* **1089,** 67-78

31. Boelens, W. C., van Boekel, M. A., and de Jong, W. W. (1998) *Biochim.Biophys.Acta* **1388,** 513-516

32. Verschuure, P., Croes, Y., van den IJssel, P. R., Quinlan, R. A., de Jong, W. W., and Boelens, W. C. (2002) *J Mol.Cell Cardiol.* **34,** 117-128

33. Boros, S., Kamps, B., Wunderink, L., de Bruijn, W., de Jong, W. W., and Boelens, W. C. (2004) *FEBS Lett.* **576,** 57-62

34. Hernandez, H. and Robinson, C. V. (2007) *Nat.Protoc.* **2,** 715-726

35. Brown, P. H. and Schuck, P. (2008) *Comput.Phys.Commun.* **178,** 105-120

36. Cole, J. L., Lary, J. W., Moody, P., and Laue, T. M. (2008) *Methods Cell Biol.* **84,** 143-179

37. Farahbakhsh, Z. T., Huang, Q. L., Ding, L. L., Altenbach, C., Steinhoff, H. J., Horwitz, J., and Hubbell, W. L. (1995) *Biochemistry* **34,** 509-516

38. Kappe, G., Aquilina, J. A., Wunderink, L., Kamps, B., Robinson, C. V., Garate, T., Boelens, W. C., and de Jong, W. W. (2004) *Proteins* **57,** 109-117

39. Sobott, F., McCammon, M. G., Hernandez, H., and Robinson, C. V. (2005) *Philos.Transact.A Math.Phys.Eng Sci.* **363,** 379-389

40. Reddy, G. B., Das, K. P., Petrash, J. M., and Surewicz, W. K. (2000) *J Biol.Chem.* **275,** 4565-4570

41. Receveur-Brechot, V., Bourhis, J. M., Uversky, V. N., Canard, B., and Longhi, S. (2006) *Proteins* **62,** 24-45

42. Benesch, J. L., Ayoub, M., Robinson, C. V., and Aquilina, J. A. (2008) *J Biol.Chem.* **283,** 28513-28517

43. Evans, P., Slingsby, C., and Wallace, B. A. (2008) *Biochem.J* **409,** 691-699

44. van Montfort, R., Slingsby, C., and Vierling, E. (2001) *Adv.Protein Chem.* **59,** 105-156

45. Sun, X., Fontaine, J. M., Rest, J. S., Shelden, E. A., Welsh, M. J., and Benndorf, R. (2004) *J Biol.Chem.* **279,** 2394-2402

46. White, H. E., Orlova, E. V., Chen, S., Wang, L., Ignatiou, A., Gowen, B., Stromer, T., Franzmann, T. M., Haslbeck, M., Buchner, J., and Saibil, H. R. (2006) *Structure.* **14,** 1197-1204

47. Zantema, A., Verlaan-De Vries, M., Maasdam, D., Bol, S., and van der, E. A. (1992) *J Biol.Chem.* **267,** 12936-12941

48. Helm, K. W., Lee, G. J., and Vierling, E. (1997) *Plant Physiol* **114,** 1477-1485

49. Sun, X., Fontaine, J. M., Rest, J. S., Shelden, E. A., Welsh, M. J., and Benndorf, R. (2004) *J.Biol.Chem.* **279,** 2394-2402

50. Reddy, G. B., Kumar, P. A., and Kumar, M. S. (2006) *IUBMB.Life* **58,** 632-641

51. Giese, K. C., Basha, E., Catague, B. Y., and Vierling, E. (2005) *Proc.Natl.Acad.Sci.U.S.A* **102,** 18896-18901

FOOTNOTES

*The authors thank Dr. Guido Kappé for helpful discussions and technical assistance. Furthermore the authors thank Carolien Vercouteren en Jurgen Ketelaars for their technical assistance. This work was supported by Grant NWO-MW 903-51-170 from the Netherlands Organization for Scientific Research to W.C.B., and by the Hungarian Eötvös Fellowship to C.S.B.

Abbreviations: sHSP: small heat shock protein, SEC: size exclusion chromatography, SDS: sodium dodecyl sulphate, EDTA: ethylenediaminetetraacetic acid, DTT: dithiothreitol, PAGE: polyacrylamide gel electrophoresis, nanoESI-MS: Nanoelectrospray ionization mass spectrometry.

FIGURE LEGENDS

Figure 1. *Separation of HSPB2/B3.* (A) **A** lysate of *E. coli* cells co-expressing HSPB2 and HSPB3 was separated on a DEAE column with a NaCl gradient. Peak samples were collected and subjected to SDS-PAGE and stained with Coomassie Brilliant Blue (CBB). (B) Elution pattern of purified HSPB2/B3 on a TSK-Gel3000SW column was measured by absorption at 280 nm (left axis) in combination with continuous MALLS measurements converted to molecular masses in Da (right axis). HSPB2/B3 eluted as relatively sharp peaks A and B at a mass of 78 kDa and 166 kDa, and a front peak C, containing multiple complexes with increasing masses.

Figure 2. *Nanoelectrospray mass spectra of HSPB2/B3.* (A) HSPB2/B3 separated by Superose 6 column in 200 mM ammonium acetate pH 6.8. Fractions of peak A and B were collected. Panel (B) shows the higher oligomeric species observed by mass spectrometry acquired with a sample of peak A. The dominant charge state series correspond to a HSPB2/B3 tetramer (T) of mass 77897 ± 34 Da composed of three 20.2 kDa subunits and a single 17.0 kDa subunit. As an insert of panel B, an expansion of the 1500 – 3500 m/z region is shown. Here, three additional species can be identified: a monomer (M) with mass 17024 ± 1 Da; a heterodimer (heteroD), with mass 37294 ± 9 Da, composed of a single copy of each subunit and a homodimer (homoD), with mass 40458 ± 39 Da, composed of two 20.2 kDa subunits. Panel (C) shows the higher oligomeric species observed by mass spectrometry, acquired with sample of peak B. The mass of the predominant charge state series in this spectrum corresponds to an octamer (O) composed of six 20.2 kDa subunits and two 17.0 kDa in the same subunit ratio observed for the tetrameric species in panel B. The next most intense peak series corresponds to that of a 24 mer with the same 3:1 subunit ratio observed previously. The insert in panel C expands the 5700 – 8000 m/z region of the spectrum. A well defined but low intensity series for a dodecameric oligomer (DoD) with mass 233767 ± 94 Da was detected as well as a low intensity series for a hexadecamer (hexD) with mass 311853 ± 19 Da. Both the dodecamer and hexadecamer conform to the same subunit ratio observed for the tetramer, octamer and 24 mer.

Figure 3. *Sedimentation velocity analysis of HSPB2/B3*. Purified HSPB2/B3 at 1.5 mg/mL in 20 mM phosphate buffer pH 7.5 containing 100 mM NaCl and 2 mM EDTA was centrifuged at 42,000 rpm in an analytical ultracentrifuge at 22 °C. A multi-species analysis of the obtained data was used to calculate the C(s) distribution of S(w).

Figure 4. *Far-UV circular dichroism spectra of HSPB2/B3.*

(A) Far-UV circular dichroism spectra (B) negative ellipticity at 204 nm of HSPB2/B3 taken after every increment of 2 °C from 20 °C till 80 °C . Dark lines in (A) indicate spectra and dark squares in (B) indicate negative ellipticity at 204 nm taken after increments of 10 °C. Protein concentration was 250 μg/mL in 10 mM potassium phosphate buffer pH 7.8.

Figure 5. *HSPB2/B3 exhibits has a low affinity for the hydrophobic probe ANS.*
The ANS binding capacity of HSPB2/B3 (□) and of αB-crystallin (●) was determined by titrating 10 μM protein with increasing ANS concentrations (plotted as molar ratio ANS/protein) and measuring intensities of the fluorescence emission maxima at the excitation wavelength set at 390 nm.

Figure 6. *HSPB2/B3 exhibits moderate chaperone-like and thermoprotective activity.* (A) Chaperone activity of 250 μg HSPB2/B3 (□) or αB-crystallin (●) determined by measuring the ability to prevent DDT-induced aggregation of 250 μg insulin at 40 °C. Insulin alone is indicated by diamonds (◆). (B) Chaperone activity of 70 μg HSPB2/B3 (□) or αB-crystallin (●) determined by measuring the ability to prevent temperature-induced aggregation of 70 μg CS at 44 °C. CS alone is indicated by diamonds (◆). (C) Thermoprotective activity of HSPB2/B3 or αB-crystallin determined by measuring the growth of *E. coli* cells expressing HSPB2/B3 (□), αB-crystallin (●) or negative control protein βB2 (◆) after a heat shock at 48 °C for 60 minutes.

Figure 7. *HSPB2 but not HSPB2/B3 interacts with HSP20*. (A) Purified HSPB2 (0.5 μg) and HSPB2/B3 (1 μg) were incubated alone (lanes 3-4) or with a mixture of HSP20, HSP27 and αB-crystallin (each 5 μg) (lanes 5-6) for 60 min at room temperature and subsequently immunoprecipitated (IP) using antibodies directed to HSPB2. As a negative control no proteins were added (lane 2). The precipitated proteins were analyzed by Western blotting using antibodies directed to the indicated proteins. Lane 1 shows 5% of the input of HSP20, HSP27 and αB-crystallin. (B) Purified HSPB2 (0.5 μg) and HSPB2/B3 (1 μg) were incubated with 5 μg HSP20 (upper panel), 5 μg HSP27 (middle panel) or 5 μg αB-crystallin (lower panel) (lanes 3-4) or with a mixture of the three proteins (each 5 μg) (lanes 5-6) for 60 min at room temperature and subsequently immunoprecipitated (IP) using the indicated antibodies. As a negative control HSPB2/B3 was incubated with buffer alone (lane 2). The precipitated proteins were analyzed by Western blotting with anti-HSPB2 serum. Lane 1 shows 5% of the HSPB2/B3 input.

Table 1. Molecular masses of the detected HSPB2/B3 oligomers as determined by nano-ESI-MS, MALLS and sedimentation analysis and compared with the calculated masses.

Multimers		Nano-ESI-MS	MALLS	Sedimentation velocity analysis (AUC)			
n-mer	Calc. Mw (Da)	Mw (Da)	Mw (Da)	Sw (20,w) (S)	Mw (Da)	Relative amount (%)	Ratio amount n+4- and n-mer
4-mer	77,673	77,897 ± 34	78,000	4.6	73,400	60.4	-
8-mer	155,346	155,696 ±53	166,000	6.9	135,000	25.4	0,4
12-mer	233,019	233,767 ± 94	-	8.8	197,000	7.9	0,3
16-mer	310,692	311,853 ± 19	-	11.1	277,000	3.1	0,4
20-mer	388,365	ND	-	13.6	376,000	0.9	0,3
24-mer	466,038	467,588 ±127	-	16.0	481,000	1.3	1,4
				19.4	638,000	0.6	-

ND: Not Detected

A

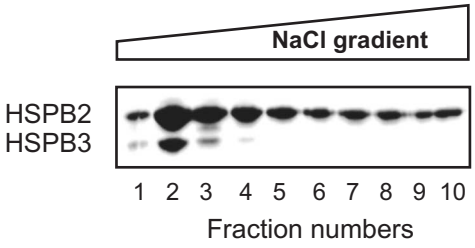
NaCl gradient
HSPB2
HSPB3
1 2 3 4 5 6 7 8 9 10
Fraction numbers

B

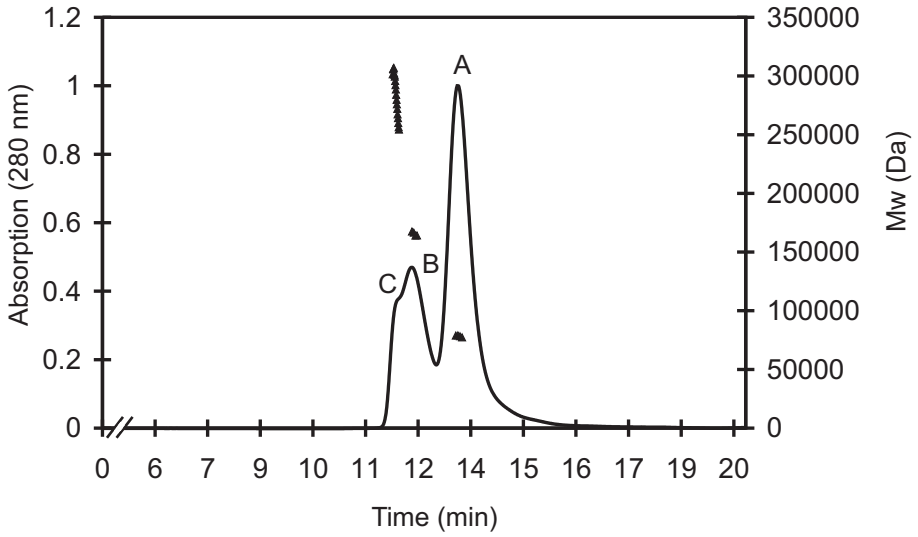
Absorption (280 nm)
1.2
1
0.8
0.6
0.4
0.2
0
A
B
C
350000
300000
250000
200000
150000
100000
50000
0
Mw (Da)
0 6 7 9 10 11 12 14 15 16 17 19 20
Time (min)

Figure 1

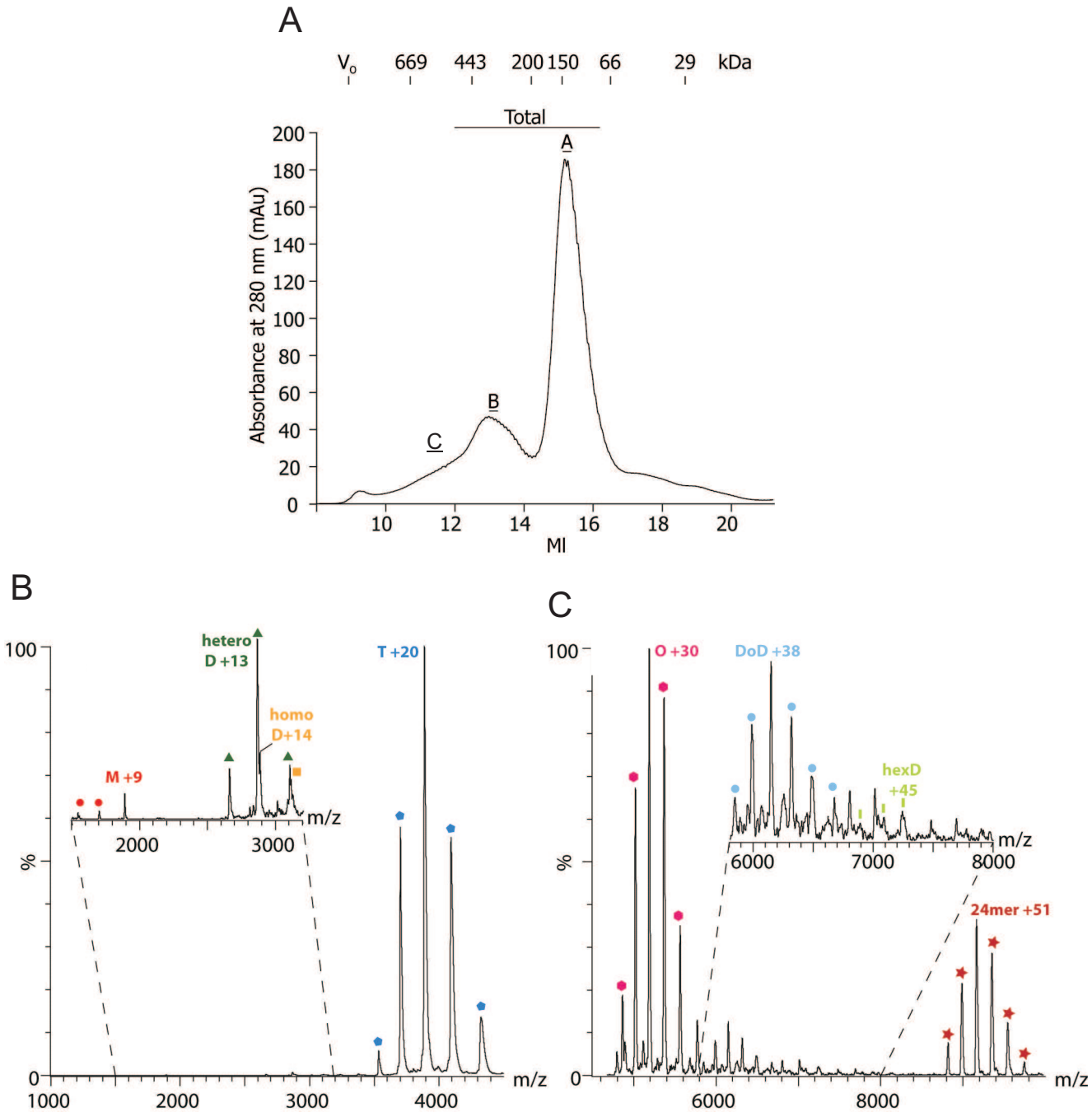
A
V0
669
443
200
150
66
29
kDa
Total
A
B
C
Absorbance at 280 nm (mAu)
MI
B
hetero
D +13
homo
D+14
T +20
M +9
m/z
%
C
O +30
DoD +38
hexD
+45
24mer +51

Figure 2

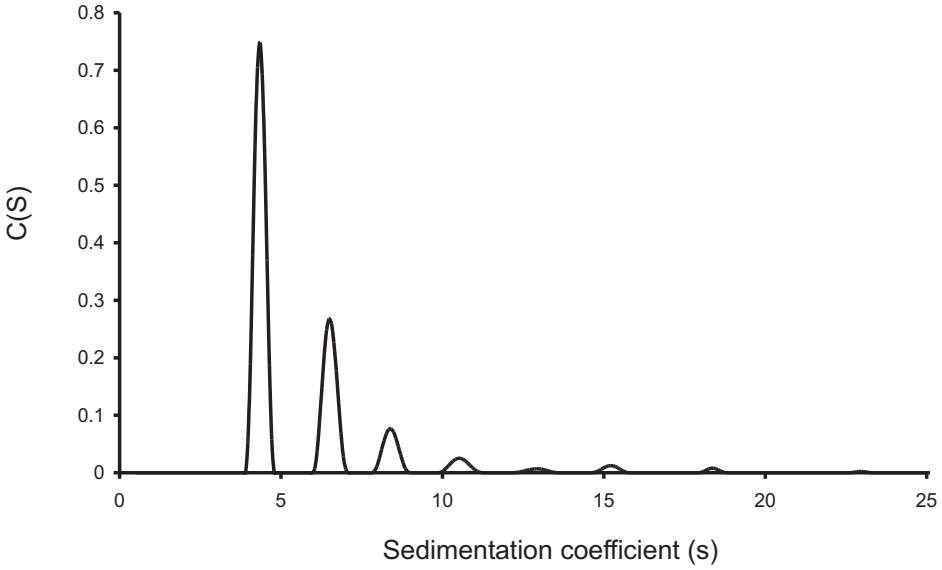
C(S)
0.8
0.7
0.6
0.5
0.4
0.3
0.2
0.1
0
0
5
10
15
20
25
Sedimentation coefficient (s)

Figure 3

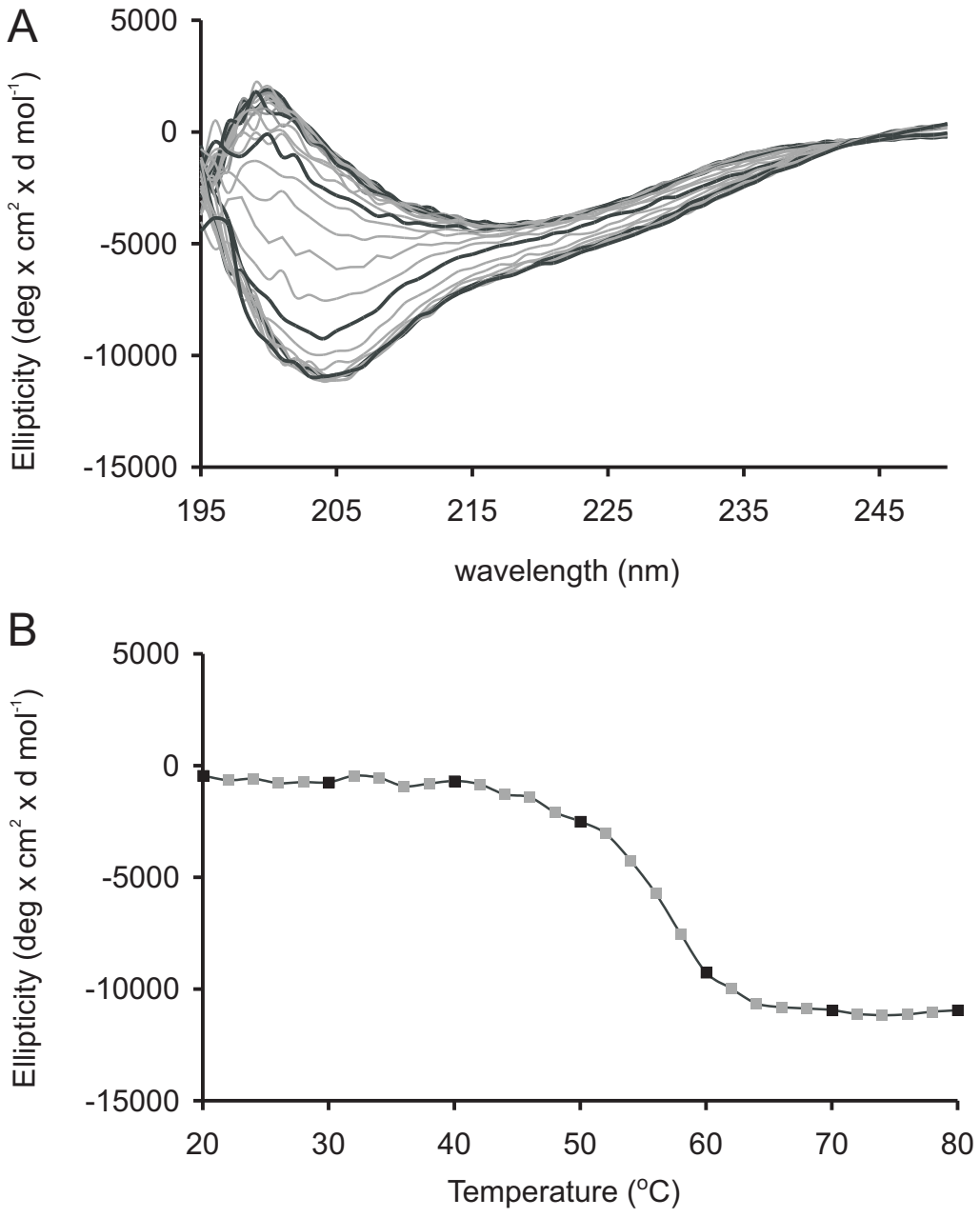
A
5000
0
-5000
-10000
-15000
Ellipticity (deg x cm^2 x d mol^{-1})
195
205
215
225
235
245
wavelength (nm)
B
5000
0
-5000
-10000
-15000
Ellipticity (deg x cm^2 x d mol^{-1})
20
30
40
50
60
70
80
Temperature (°C)

Figure 4

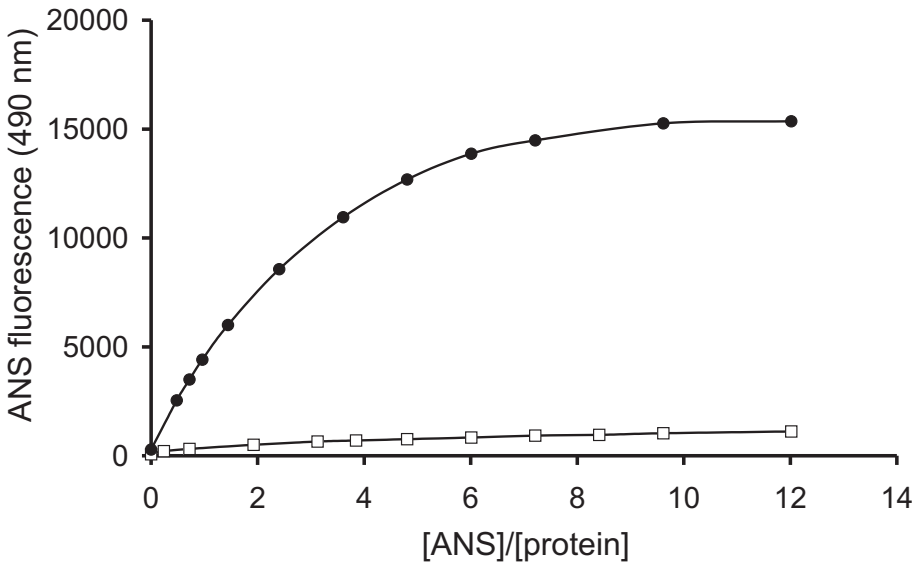
ANS fluorescence (490 nm)
20000
15000
10000
5000
0
0
2
4
6
8
10
12
14
[ANS]/[protein]

Figure 5

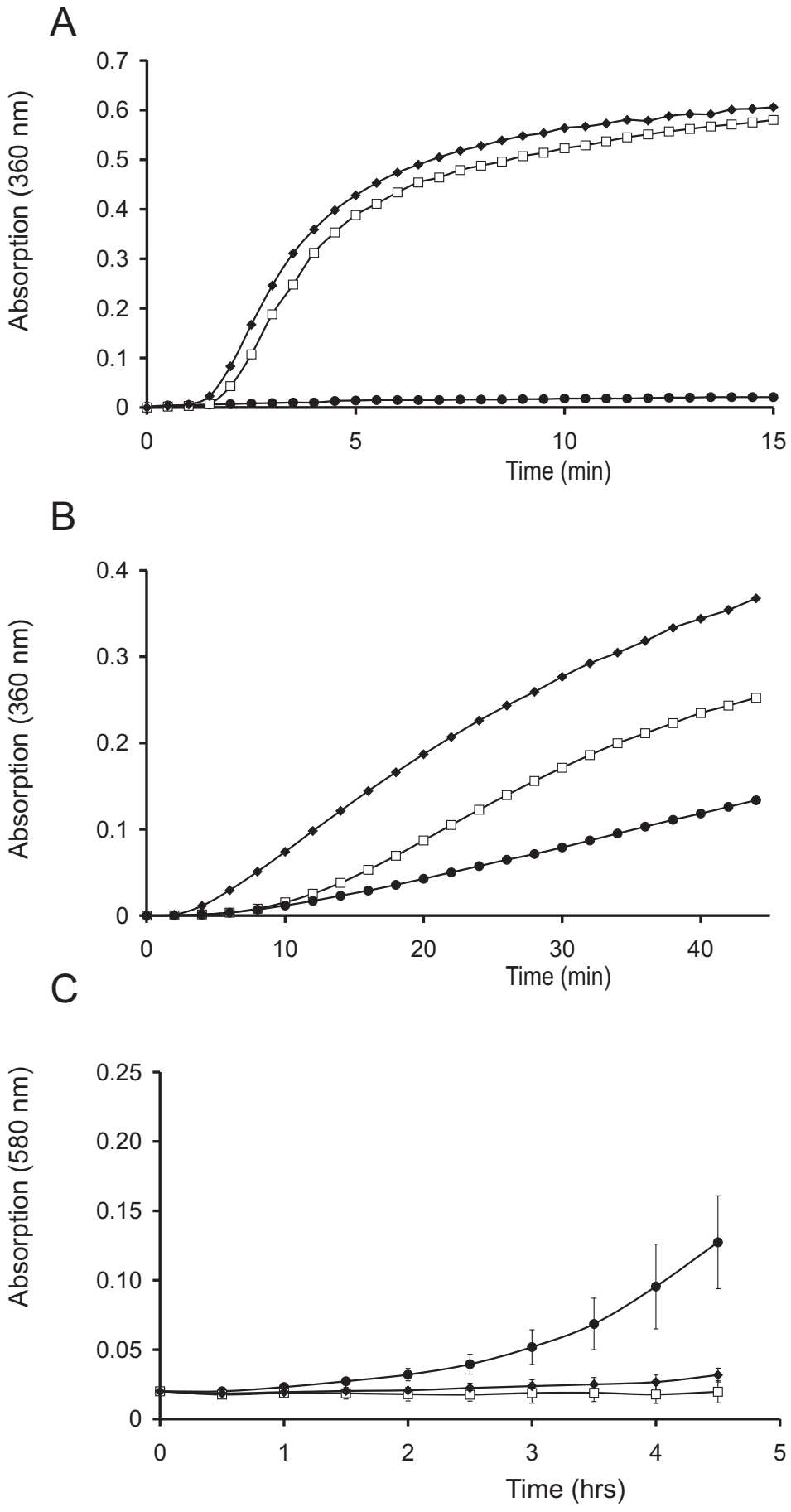
A
Absorption (360 nm)
0.7
0.6
0.5
0.4
0.3
0.2
0.1
0
0
5
10
15
Time (min)
B
Absorption (360 nm)
0.4
0.3
0.2
0.1
0
0
10
20
30
40
Time (min)
C
Absorption (580 nm)
0.25
0.20
0.15
0.10
0.05
0
0
1
2
3
4
5
Time (hrs)

Figure 6

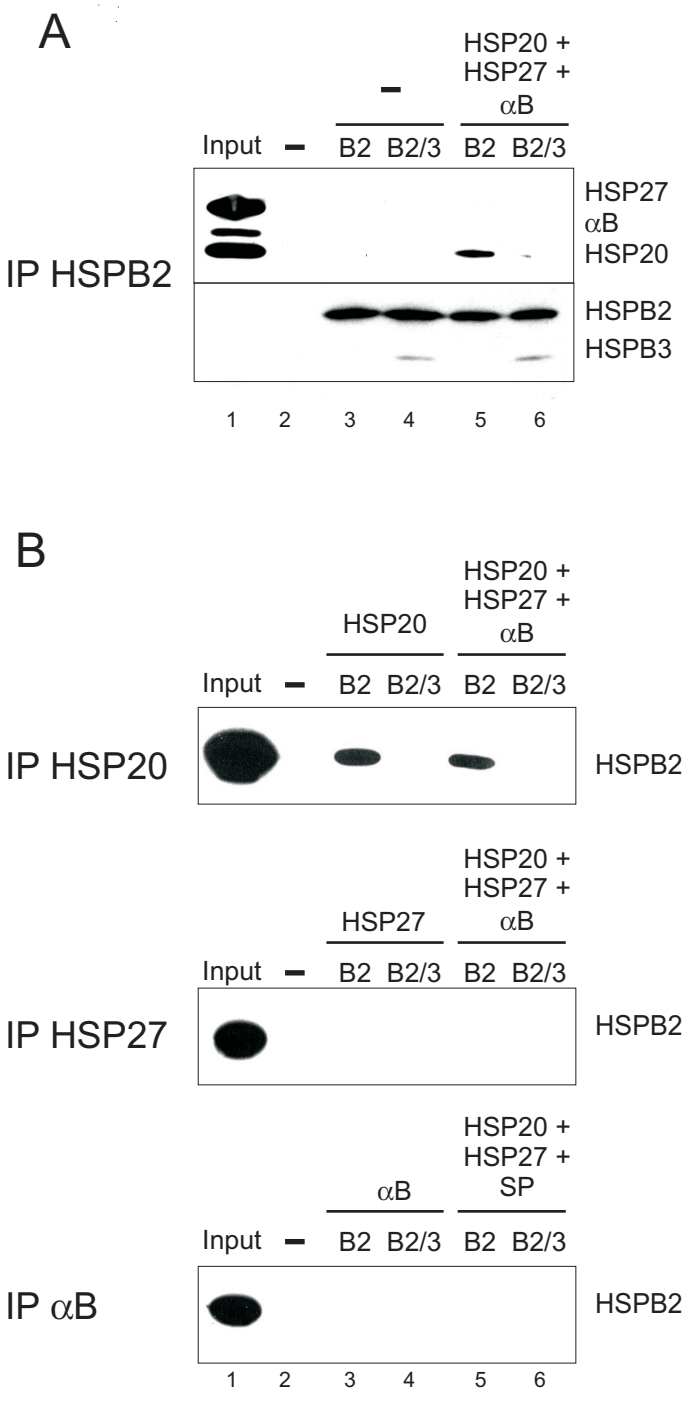
A
HSP20 +
HSP27 +
αB
–
Input – B2 B2/3 B2 B2/3
IP HSPB2
HSP27
αB
HSP20
HSPB2
HSPB3
1 2 3 4 5 6
B
HSP20 +
HSP27 +
αB
HSP20
Input – B2 B2/3 B2 B2/3
IP HSP20
HSPB2
HSP20 +
HSP27 +
αB
HSP27
Input – B2 B2/3 B2 B2/3
IP HSP27
HSPB2
HSP20 +
HSP27 +
SP
αB
Input – B2 B2/3 B2 B2/3
IP αB
HSPB2
1 2 3 4 5 6

Figure 7